



Antineutrino flux from the EDF Hartlepool nuclear power plantSandra Bogetic *†‡§*University of Tennessee, Knoxville, Tennessee 37996, USA*Robert Mills †‡§*United Kingdom National Nuclear Laboratory, Central Laboratory, Sellafield, Seascale, Cumbria CA20 1PG, United Kingdom*Adam Bernstein §*Lawrence Livermore National Laboratory, Livermore, California 94550, USA*Jonathon Coleman[§] and Alex Morgan*University of Liverpool, Liverpool L69 7ZE, United Kingdom*Andrew Petts *EDF Energy, Barnett Way, Barnwood, Gloucester GL4 3RS, United Kingdom* (Received 19 January 2023; revised 21 May 2024; accepted 22 May 2024; published 21 June 2024)

In this paper, we present a detailed simulation of the antineutrino emissions from an advanced gas-cooled reactor (AGR) core, benchmarked with input data from the United Kingdom Hartlepool reactors. An accurate description of the evolution of the antineutrino spectrum of reactor cores is needed to assess the performance of antineutrino-based monitoring concepts for nonproliferation, including estimations of the sensitivity of the antineutrino rate and spectrum to fuel content and reactor thermal power. The antineutrino spectral variation we present, while specific to AGRs, are different from studies published previously and help provide insight into the likely behavior of other reactor designs that use a similar refueling approach, such as those used in the RBMK (реактор большой мощности канальный – “high-power channel-type reactor”), CANDU (Canada Deuterium Uranium), and other reactors.

DOI: [10.1103/PhysRevApplied.21.064051](https://doi.org/10.1103/PhysRevApplied.21.064051)**I. INTRODUCTION**

Nuclear reactors have been successfully used as a source of electron antineutrinos in numerous antineutrino physics experiments [1,2] and have been proposed for use in safeguards applications [3–5]. Reactors have played a central role in characterizing antineutrino oscillations, due to their high intensity and reasonably well predicted antineutrino emission spectrum. The spectral prediction is essential for some monitoring applications and fundamental studies of antineutrino properties. For example, the spectral evolution can be used to estimate reactor characteristics such as fuel burn-up and time-averaged power [3], as well as to facilitate the estimation of fundamental properties of the antineutrino, such as mixing angles [6].

Antineutrinos arise from beta decays of fission-product daughters, with an average number of decays (and thus antineutrinos) of about three per daughter and six per fission. The total number of antineutrinos per fission event varies only modestly with fissile isotope. However, the population of daughters varies considerably among these isotopes, resulting in substantial differences in the emitted antineutrino energy spectrum for each. To predict the spectrum, the number of fissions arising from each parent isotope—which varies in time over the course of the reactor cycle—must be calculated. In this paper, we perform this calculation through the use of an assembly-level simulation of the core, which is used to track the evolution of fission rates from each isotope throughout the cycle. Antineutrino spectra at each instant in the cycle can then be derived by convolving the fission rates with the tabulated number of antineutrinos per unit of energy per fission [7].

Other authors have made similar estimates for pressurized-water reactors (PWRs) fueled with low-enriched uranium [8], mixed-oxide assemblies [9], Canada Deuterium Uranium (CANDU) reactors [10], and

*Corresponding author: sbogetic@utk.edu†Corresponding author: robert.w.mills@uknln.com

‡coauthor

§WATCHMAN Collaboration

thorium-fueled reactors [11]. The prediction presented in this paper for an advanced gas-cooled reactor (AGR) are different from previously published studies of other reactor types. A key finding is that the relatively short (approximately 4-month) refueling intervals and relatively small (approximately 6% of the core per outage) fuel-replacement fraction contribute to a smaller change in the antineutrino flux and spectrum from beginning to end of cycle compared to other reactor types.

II. HARTLEPOOL ADVANCED GAS-COOLED REACTORS

In the United Kingdom (UK), Germany, and the United States, gas-cooled reactors have been in operation for many years. Specifically, in the UK, nuclear electricity has mostly been generated by CO₂-cooled magnesium non-oxidising (MAGNOX) reactors and AGRs since the 1980s. The AGR considered for the antineutrino prediction study in this paper is the Hartlepool nuclear power plant (NPP). The choice of the Hartlepool reactors has been driven by the collaboration effort with the reactor engineers to get reactor operational data for the antineutrino study. This has allowed for a high-fidelity calculation of the reactors fractional fission rates (FFRs) for the most important fissioning nuclides in the reactors and to further the sensitivity study of the antineutrino flux on the level of fidelity of the reactor simulations.

A. Reactor station description and operation

Hartlepool Power Station is located on the north-east coast of England and has been safely producing low-carbon electricity since 1983. The power station operates two AGRs. The AGR design at Hartlepool Power Station consists of a graphite-moderated reactor core and uses pressurized CO₂ as the primary coolant. The active core has a mean diameter of approximately 9.3 m and a height of 8.2 m, while the total core has a diameter of approximately 11.9 m and a height of 12.7 m. The reactor core consists of columns of circular-cross-section graphite bricks with interstitial square-cross-section graphite bricks. There are 324 on-lattice fuel channels formed by bores in the larger circular bricks. Each bore is 0.27 m in diameter and is pitched at approximately 0.47 m. There are 81 control-rod channels in a one-in-four array in the smaller square brick columns. Within each of the 324 fuel channels are eight stacked fuel elements, each containing 36 clustered fuel pins arranged in concentric rings of 18, 12, and 6 pins, within a graphite sleeve. The stainless-steel fuel pins are approximately 1 m in length with a diameter of 14.48 mm and contain stacked ceramic UO₂ pellets of either 3.2% or 3.78% ²³⁵U. The total core inventory of uranium is approximately 130 tonnes. The primary coolant is driven around the core by eight gas

circulators, each of which has a constant-speed motor running at 3000 rpm, resulting in a total gas mass flow of 3600 kg s⁻¹. In normal full-power operation, the primary coolant operates at 39 bar with temperatures at the bottom of the active core around 543 K and at the top of the active core 923 K. Heat is deposited into eight steam generators by the pressurized CO₂. Demineralized water acts as the secondary coolant and is fed to each steam generator in a closed-loop system at a rate of 60 kg s⁻¹. The primary and secondary loops are separated within the steam generator to ensure that no contamination is spread to the steam-side equipment from the active primary coolant. The steam generators operate at approximately 139 bar and produce steam at 843 K, resulting in an output of around 1560 MWth and 600 MWe for each reactor.

Fuel typically remains in the cores for around 8 years, with an average discharge irradiation of 32 GWd/T_e. On-load average fuel irradiation is around 15.5 GWd/T_e. The reactors typically remains at full power for 20–22 weeks before undergoing a controlled reactor shut down for off-load depressurized batch refueling, where around 20 of the highest-burn-up fuel assemblies are replaced. The reactors remain shut down during these periods for around 10–14 days, after which they returns to full-power operation over a period of a 2–3 days. Outages across the two reactors are staggered to avoid overlap of shut-down periods. This results in five shut-down periods per year across the two reactors.

B. PANTHER simulation of the full core

Full operational data for both Hartlepool reactors have been obtained, including the power history, the fuel-element irradiation (MWd/t_e), the power rating (MW/t_e), the initial enrichment, and the loading dates for the whole core over a 12-month operational period. The reactor power for each core has been calculated using the thermal-hydraulics code HEYPEX. The HEYPEX code calculates reactor power based on plant measurements of coolant mass flow and inlet and outlet reactor core temperatures. The thermal-neutronics code PANTHER has been used to calculate individual fuel-element powers and irradiations as part of the Core Follow Regular Assessment Route. The Regular Assessment Route is executed approximately weekly and provides a steady-state assessment against various reactor compliance limits. A fixed three-dimensional (3D) reactor model describing the reactor geometry, materials, and basic nuclear data is imported into the calculation route. The reactor model consists of one mesh point per reactor channel, providing 324 radial points. Axially, the reactor model consist of eight mesh points, one per fuel element. Measured plant parameters such as control-rod positions, the reactor thermal power, the fuel-channel inlet and outlet temperatures, and the coolant mass flows are imported along with the 3D reactor state from the previous

Regular Assessment, which is used as a calculation starting point. Individual element powers, irradiations, and decay heat-source terms are then calculated using the thermal-neutronic model to solve a steady-state diffusion equation approximation.

C. Prediction of fission rates using FISPIN

The Schreckenbach measurements reported in 1981, 1982, and 1989 [12] showed little change in the emitted beta spectra from the neutron irradiation of pure actinide samples after 20–30 h. It has been assumed that the beta emission is dominated by short-lived fission products that, for the case of a constant fission rate of a specific nuclide, will quickly produce an equilibrium concentration of the resultant fission products and thus a time-independent spectrum thereafter. More recently, Huber [7] has used these measured spectra and observations to assume that the neutrino emission of reactors can be represented by an antineutrino spectra for each nuclide that has been fissioned. Thus if you know the fission rates for each principal fissionable nuclide, you can use these to weight the time-independent antineutrino spectra per fission to produce an antineutrino emission spectrum from a reactor.

In previous work, Mills *et al.* [13] have used the UK reactor modeling code WIMS and the UK spent-fuel inventory code FISPIN to model the change in fission rates in nuclear fuel with burn-up for typical initial enrichment, reactor power, and burn-up values for PWRs, boiling-water reactors (BWRs) and AGR reactors in a fuel assembly. These results have been published as a database in MENDELEY DATA [14].

For a specific reactor type, it is therefore possible to interpolate the fission rates in a reactor assembly based upon initial enrichment, burn-up, and power. From the fission fractions, the average energy release per fission can then be determined and thus the total number of fissions estimated for a given power. If these data are available for all the fuel assemblies in a reactor, the total antineutrino source can be determined using the Huber antineutrino spectra for each fissioning nuclide per fission.

D. Antineutrino rate

Here, antineutrinos from the Hartlepool reactors are detected via the inverse-beta-decay (IBD) interaction [7,15]. In this process, antineutrinos interact with quasifree protons in the water, producing a positron-neutron pair in the final state:

$$\bar{\nu}_e + p \rightarrow e + n. \quad (1)$$

The positron is detected as a prompt signal through the Cherenkov light emitted when the particle velocity exceeds the speed of light in the water. This is a coupled threshold reaction in which the antineutrino energy must

exceed 1.8 MeV to generate an IBD reaction and the resulting positron kinetic energy must exceed approximately 253 keV in water to generate Cherenkov light. The neutron produced through IBD will elastically scatter off hydrogen in the detector until thermalization, after which it can be captured on either a gadolinium or a hydrogen nucleus. Following gamma-ray production from neutron captures, Cherenkov light is emitted through the Compton scattering on electrons. Due to the threshold required for Cherenkov emission, not all of the scattered electrons from gamma rays released from neutron capture on Gd will contribute to the signal. From there, the individual events have been sampled based on the reactor thermal power and the stand-off from the detector, L . The expected antineutrino flux $N(E_{\bar{\nu}}, L)$ detected in the detector is given by

$$N(E_{\bar{\nu}}, L) = \frac{n_p T}{4\pi L^2} \sum_l N_l^f \phi_l(E_{\bar{\nu}}) \sigma(E_{\bar{\nu}}) P_{ee}(E_{\bar{\nu}}, L). \quad (2)$$

where n_p refers to the number of quasifree protons and T is the counting time of the experiment. The electron antineutrino survival probability due to oscillations and the inverse-beta-decay cross section are given by P_{ee} and σ , respectively [7]. The individual contributions of fissile isotopes l are represented by the fissile fraction for the specific isotope, N_l^f , and the unique spectrum for that isotope, ϕ_l , which is assumed to follow the approximations taken from Ref. [7].

Neglecting contributions from the background, the measured antineutrino signal will be governed by the position, burn-up, and power of the Hartlepool NPP. The analysis assumes the following energy-per-fission contributions, used by FISPIN: ^{235}U , 201.7 MeV per fission; ^{238}U , 205.0 MeV per fission; ^{239}Pu , 210.0 MeV per fission; and ^{241}Pu , 212.9 MeV per fission.

III. HARTLEPOOL ANTINEUTRINO EMISSION ESTIMATION

The reactor information supplied by EDF Energy includes the burn-up (GWd/t), power (MW/t), and initial enrichment ($^{235}\text{U}:\text{U}$ weight percentage) for each of the 2592 assemblies in both reactors at a selection of times during the 2020 calendar year, as well as the total thermal-reactor power (MW) during this period. Thus the antineutrino emission from each assembly can be determined and combined to produce an antineutrino emission spectrum for each reactor. Note that you must calculate the emission for each assembly and combine these before recalculating the fission fractions from the total to give core average values, as the energy per fission will vary differently during burn-up in each assembly.

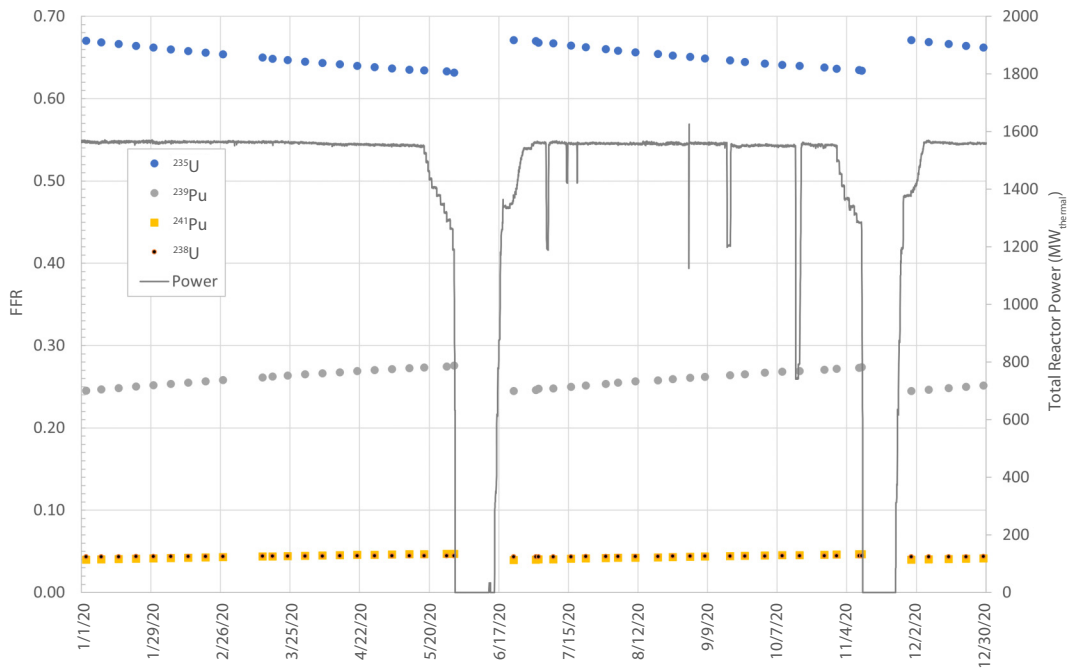


FIG. 1. The FFRs for Hartlepool reactor unit 1 in 2020.

The reported reactor power over calendar year 2020 and the estimated variation of the total core fission fractions are shown in Figs. 1 and 2 for the two units. It should be noted that approximately 12% of the assemblies in the core are changed during shut downs approximately every 6 months, so that the FFRs in the locations of replaced fuel are reset to the value of zero burn-up at these times. The frequent refueling of a small fraction of the core results in the FFRs

varying less than reactors that change a greater fraction of the core yearly or less frequently.

A. Antineutrino rate for Hartlepool

The distance for which the neutrino rate is simulated is 26 km, which also represents the distance between the Hartlepool AGR and the STFC Boulby Underground

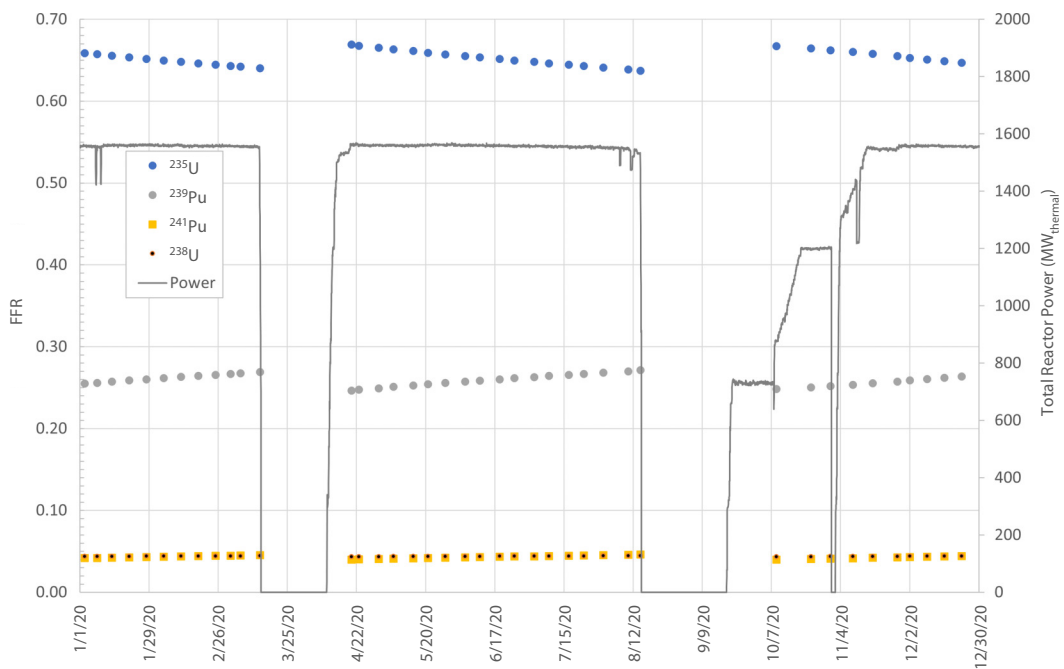


FIG. 2. The FFRs for Hartlepool reactor unit 2 in 2020.

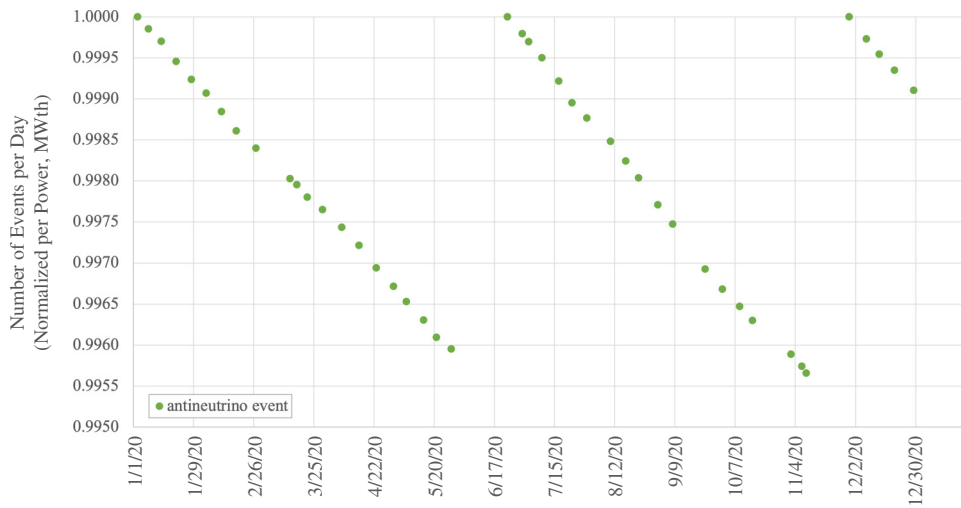


FIG. 3. The total antineutrino flux per reactor per fuel-cycle length (days) for Hartlepool AGR unit 1 in 2020.

Laboratory, the low background of which, at 1100 m depth, could simplify antineutrino measurements at distance. In Figs. 3 and 4, we show the antineutrino rates for cores 1 and 2. The values of the normalized antineutrino rates from Figs. 3 and 4 are listed in Tables I and II.

As shown in Figs. 3 and 4, the antineutrino flux decreases, over the reactor cycle, with burn-up, in accordance with low-enriched uranium (LEU) reactors. This is due to increased production of and reliance on ^{239}Pu , which emits fewer antineutrinos per fission above the inverse-beta detection threshold. On the other hand, the detected antineutrino rate is seen not to decrease significantly, due to the short reactor cycle and the lower-discharge burn-up. In Fig. 5, we present the spectral shapes of the antineutrino rates against energy at the beginning (BOC), on day 1, in the middle (MOC), on day 80, and at the end of the cycle (EOC), on day 160 of operation for Hartlepool AGR unit 1. As expected, there is no evident difference in the shape

or intensity among the spectra from BOC to EOC. Only the combined effects of power and burn-up are constrained by the measured antineutrino-rate evolution. Similar results are expected for Hartlepool AGR unit 2 since, per cycle, the FFR (Fig. 1) and the reactor power are the same as in unit 1.

IV. DISCUSSION: LESSONS LEARNED FOR DETECTION OF REACTOR NEUTRINOS

A. Rate from full-core analysis versus simplified model

The possibility of having full-core operational data, for a year of operation, has given us the unique possibility to calculate high-fidelity antineutrino rates for a full-cycle evolution and to determine the sensitivity of the antineutrino evolution to the reactor full-core operation calculation. In practice, the antineutrino emission from a reactor depends on the 3D distribution of fission rates throughout the core.

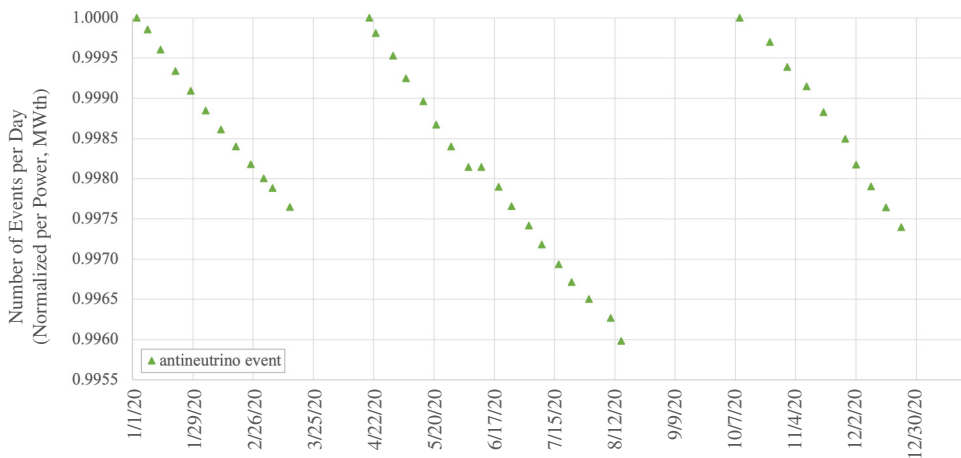


FIG. 4. The total antineutrino flux per reactor per fuel-cycle length (days) for Hartlepool AGR unit 2 in 2020.

TABLE I. The number of antineutrino events per fully operational day per MegaWatt (MW_{th}) normalized to BOC for Hartlepool AGR unit 1 in 2020.

Date	Unit 1
1/3/20	1.00000000
1/8/20	0.99986048
1/14/20	0.99968778
1/21/20	0.99947408
1/28/20	0.99923388
2/4/20	0.99903646
2/11/20	0.99885671
2/18/20	0.99865693
2/27/20	0.99842362
3/14/20	0.99802671
3/18/20	0.99794446
3/24/20	0.99776692
3/31/20	0.99761623
4/7/20	0.99742975
4/14/20	0.99721036
4/23/20	0.99695111
4/30/20	0.99672181
5/5/20	0.99653244
5/15/20	0.99629325
5/21/20	0.99612386
5/27/20	0.99596446
6/23/20	1.00000000
6/30/20	0.99979292
7/3/20	0.99969994
7/10/20	0.99950296
7/16/20	0.99927275
7/23/20	0.99898309
7/30/20	0.99875836
8/11/20	0.99844677
8/20/20	0.99820009
8/26/20	0.99802333
9/2/20	0.99769677
9/8/20	0.99746010
9/22/20	0.99695379
10/1/20	0.99664722
10/9/20	0.99643354
10/16/20	0.99622684
11/1/20	0.99588338
11/7/20	0.99571558
11/9/20	0.99562975
11/30/20	1.00000000
12/7/20	0.99973995
12/15/20	0.99952325
12/22/20	0.99926661
12/29/20	0.99905990

These parameters themselves depend on the fuel composition and neutron flux within the core. This has required a detailed burn-up analysis of the reactor, including knowledge of the fuel placed within the core with its design, including the initial composition, and operational parameters, as well as the temperatures of the fuel and coolant and the reactor thermal power. In practice, this is information

TABLE II. The number of antineutrino events per fully operational day per MegaWatt (MW_{th}) normalized to BOC for Hartlepool AGR unit 2 in 2020.

Date	Unit 2
1/3/20	1.00000000
1/8/20	0.99985512
1/14/20	0.99960319
1/21/20	0.99933942
1/28/20	0.99909271
2/4/20	0.99884680
2/11/20	0.99860989
2/18/20	0.99839880
2/25/20	0.99817993
3/2/20	0.99800270
3/6/20	0.99788276
3/14/20	0.99764920
4/20/20	1.00000000
4/23/20	0.99980961
5/1/20	0.99952897
5/7/20	0.99924657
5/15/20	0.99896438
5/21/20	0.99867358
5/28/20	0.99840161
6/5/20	0.99814455
6/11/20	0.99814455
6/19/20	0.99789986
6/25/20	0.99765662
7/3/20	0.99741685
7/9/20	0.99717992
7/17/20	0.99693599
7/23/20	0.99671767
7/31/20	0.99650674
8/10/20	0.99626922
8/15/20	0.99598243
10/9/20	1.00000000
10/23/20	0.99970068
10/31/20	0.99938939
11/9/20	0.99915044
11/17/20	0.99882932
11/27/20	0.99849365
12/2/20	0.99817474
12/9/20	0.99790525
12/16/20	0.99764353
12/23/20	0.99739683

that is only known to those modeling the reactor to support operation and it is seldom distributed to others.

For this study, we have been able to perform a comparison using a simplified model of a Hartlepool AGR, the Sizewell B PWR, and the San Onofre PWR operations. These PWRs have been chosen as they use different refueling strategies but similar fuels. The approximation used is that the core consists of a number of fuel batches that, when inserted, have zero burn-up, but the accumulated burn-up is according to the average power of the reactor. So if the core consists of N batches of fuel, each batch would have a different burn-up, depending on the number

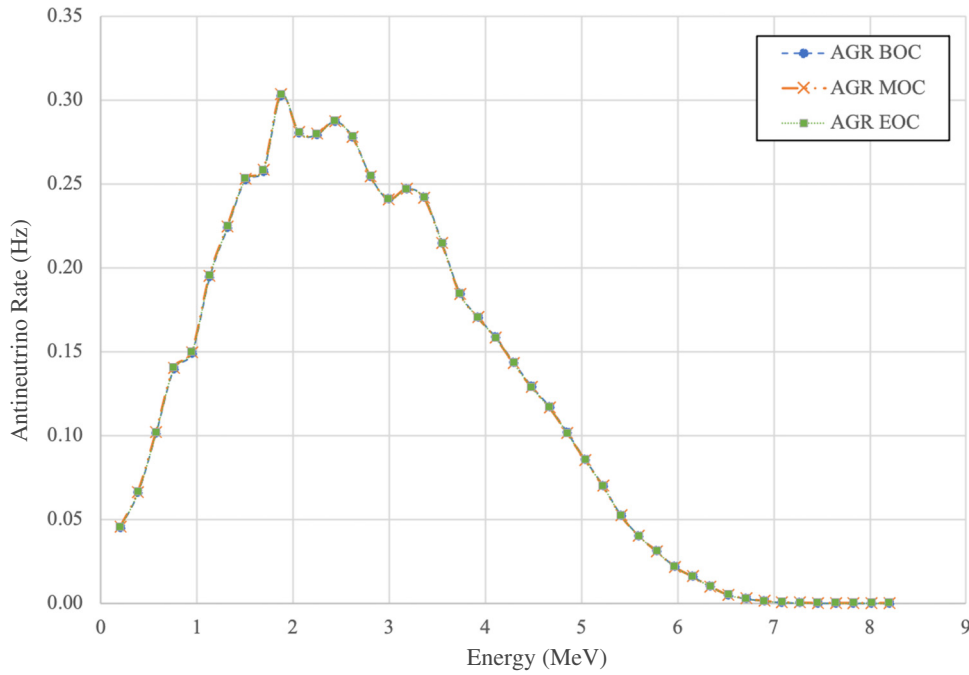


FIG. 5. Spectrum of antineutrino rates over energy (MeV) along three points in the reactor fuel cycle (days 1, 80, and 160) for Hartlepool AGR unit 1. The three curves overlap, with no noticeable differences.

of cycles during which it has been in the core. The FFRs can be determined at start-up following a fuel replacement for each batch and then during the period until the reactor is shut down for the next fuel replacement. Using the available data in Table III, the changes of the antineutrino emission have been calculated and are shown in Fig. 6. The AGR shows less variation with its more frequent refueling, with the yearly and 2-yearly PWR showing a much more pronounced variation. It is noted that any independent calculation previously reported using the CASMO-SIMULATE package gives very similar results to this simplified method using the WIMS-FISPIN FFRs based upon different nuclear data libraries.

B. Antineutrino flux comparison AGR versus PWR

It is of interest for the sake of studying the sensitivity of the antineutrino rate for various types of NPPs to compare the flux from an AGR to that from a light-water reactor (LWR) commonly used around the world. The reactor chosen for the comparison is the San Onofre Nuclear Generating Station (SONGS) NPP and the resulting antineutrino flux rate is from the SONGS detector experiment. The SONGS1 detector [13] was operated at the SONGS reactor between 2003 and 2006. The active volume comprised 0.64 tons of Gd-doped liquid scintillator contained in stainless-steel cells. The detector was

TABLE III. Reactor information from the World Nuclear Industry Handbook 2003 [16].

Quantity	San Onofre 2	Sizewell	Hartlepool 1
Reactor type	PWR	PWR	AGR
Enrichment (wt% $^{235}\text{U}/\text{U}$)	3.97 ^a	3.1	3.1
Initial mass of uranium in the core (tons)	89.5	88.6	110
Thermal-reactor power (MW)	3390	3411	1550
Average rating (MW/t)	37.9	38.5	14.09
(thermal power divided by initial mass of uranium)			
Length of cycle (months)	24	12	4
Typical shut down between cycles (days)	60	40	14
Percentage of fuel mass changed at refueling (%)	49.5	33	7.3
Typical number of cycles for which fuel is in the core, N (approximated to the nearest integer)	2	3	14
Average burn-up of spent fuel discharged (GWd/t)	33	33	24

^aValue not available for San Onofre 2; value used from sister station San Onofre 3.

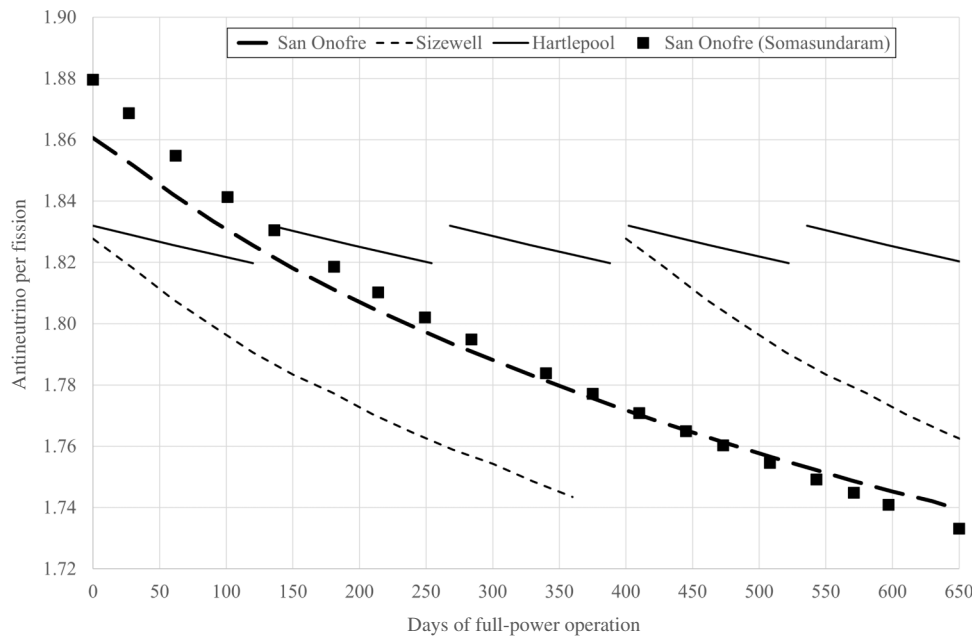


FIG. 6. Variation of the average detectable antineutrinos per fission event from the Hartlepool, Sizewell, and San Onofre reactors, calculated using the simplified method convoluted with the Huber [7] number of neutrinos emitted per fission over the IBD threshold of 1.8 MeV. The convolution of the detailed whole-core model results using the CASMO-SIMULATE package [17,18] is shown by the square markers.

located in the tendon gallery of one of the two PWRs at SONGS, about 25 m from the reactor core. As for most operating PWRs, SONGS has LEU cores with a mixture of fissions— ^{235}U approximately 55%, ^{239}Pu approximately 30%, ^{238}U approximately 10%, and ^{241}Pu approximately 5%—a large power output (approximately 3 GWth) and a long fuel-cycle length before refueling approximately every 600 days. For the sake of comparison, the SONGS PWR reactor is considered at the same 26-km distance as Hartlepool/Boulby to allow for distance and neutrino

oscillation effects. As well as the comparison seen in Figs. 7 and 8, the difference in the flux along the cycle has been normalized to the initial flux for both cases (AGR versus PWR).

Under standard operation of both the PWR and the AGR, the antineutrino flux rate from primarily fissioning ^{235}U to ^{239}Pu can be tracked and is in line with reactor observations. Changes in the antineutrino flux throughout an actual AGR fuel cycle and over a whole year are within 1%, compared to PWR changes of almost 10%.

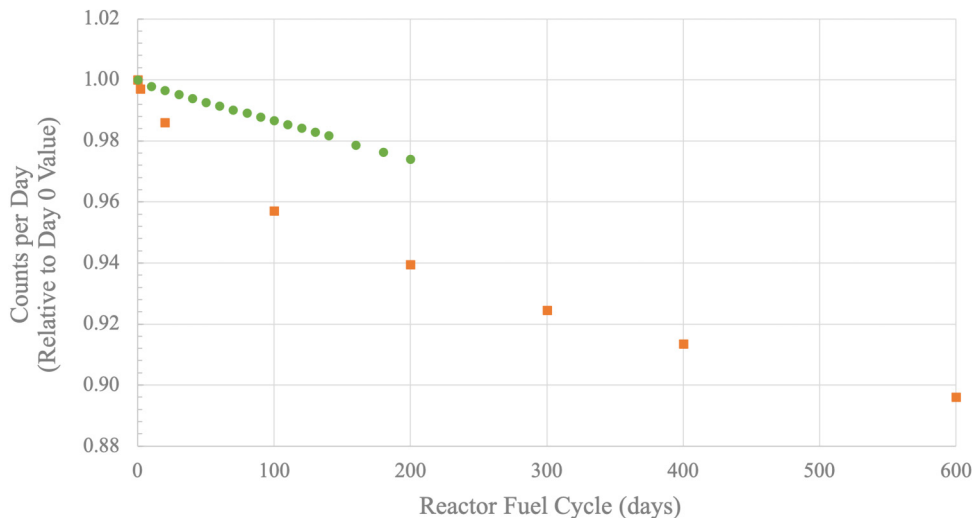


FIG. 7. The antineutrino flux rate for Hartlepool reactor unit 2 and the SONGS NPP.

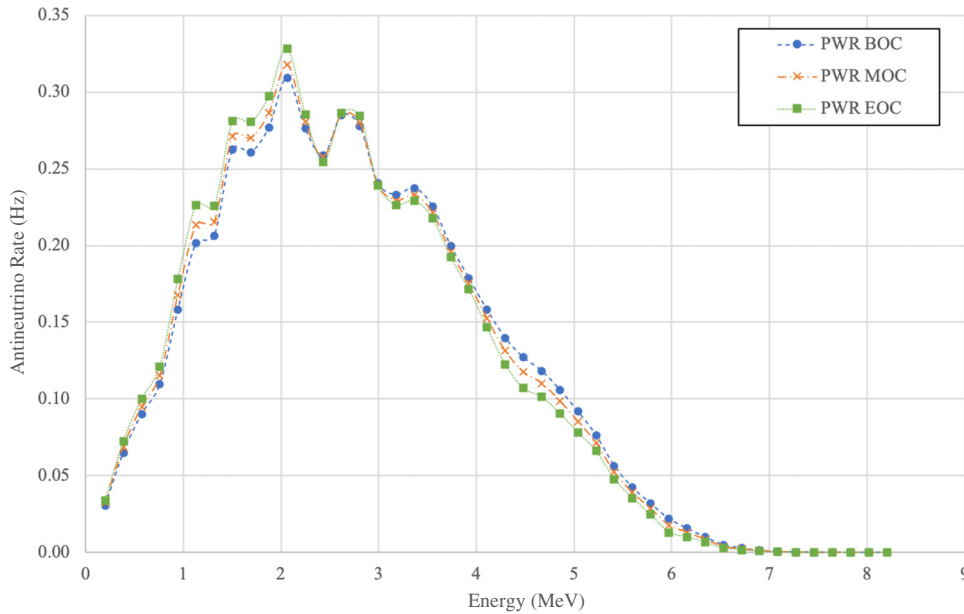


FIG. 8. The spectral result of antineutrino rates against energy (MeV) at three points in the reactor fuel cycle (days 1, 800, and 1600) for the SONGS reactor unit.

Also, changes in the FFR of ^{235}U and ^{239}Pu are not significant in the AGR due to the smaller fraction of fuel being replaced more regularly. The shorter fuel cycle of the AGR, compared to the PWR (210 versus 600 days) is a key factor for a low antineutrino-rate change from BOC to EOC, given the lower power of approximately 1500 MWth for the AGR, versus approximately 3 GWth for the SONGS PWR.

V. FUTURE OF REACTOR MONITORING

Though only operated in the UK, the AGR, with its batch-refueling regime, is similar in operation to other reactor designs that employ on-load small-batch refueling, such as the реактор большой мощности канальный – “high-power channel-type reactor” (RBMK), CANDU, MAGNOX, Uranium Naturel Graphite Gaz (UNGG), and быстрый натрий (BN – “fast sodium”) series fast-breeder reactors. One could therefore expect a similar antineutrino profile from such reactor designs. It is also worth noting that more exotic reactor designs, such as pebble-bed and some Generation-IV reactors, also employ a similar on-load refueling regime.

It is known that plutonium production favors low-burn-up early discharge fuel and that the RBMK and MAGNOX reactor designs were developed in part for their ability to produce significant quantities of weapons-grade plutonium. More modern conventional reactor designs favor steady operation over extended periods to maximize electricity generation, or capability factor and fuel utilization. Changes to the observed antineutrino profile could potentially be used to infer changes in refueling strategy,

with a flatter profile inferring more frequent refueling and discharging of low-burn-up fissile material. This has the potential to act as a verification tool to ensure that operators of nuclear facilities are declaring accurate fuel loading and discharge information for nuclear safeguarding.

The information can be inferred from the measured antineutrino flux: in order to make reliable conclusions about reactor operations and fuel loadings, burn-up and reactor power must be decoupled. The reported reactor power could be used for this purpose, although is susceptible to falsification. Radioisotope emissions and isotopic ratios could potentially be used to infer reactor power, as certain key short-lived isotopes of xenon and krypton are produced *pro rata* with the reactor load and are approximately independent of burn-up. This information could therefore help interpret any observed changes in the antineutrino profile. The XENAH project [19] currently in operation at Hartlepool Power Station is measuring isotopic emissions both at source and remotely. Data from this project could provide valuable contextual information to either of the calculated antineutrino profiles reported in this work, or in future observed antineutrino profiles as measured by a detector deployed close to the source.

VI. SUMMARY AND CONCLUSIONS

In this paper, we have presented a detailed simulation of the antineutrino emissions from an AGR core, benchmarked with input data from the UK Hartlepool reactor showing differences with other reactors previously modelled. The Hartlepool operational data were provided to us for a full 12-month refueling and outage cycle and

this information has been used as an input to the thermal-hydraulics code HEYPEX and the thermal neutronics code PANTHER, to calculate the overall reactor power and the assembly-level power and burn-up, respectively. The emitted antineutrino spectra per fission and isotope are based on the Huber-Muller parametrization. These isotope-specific spectra are weighted by the number of fissions for each isotope, then summed to obtain an aggregate spectrum. The summed antineutrino spectrum evolves throughout the cycle due to the changing quantities of fissile isotopes in the core.

One of our main findings is that the relatively short (approximately 4-month) refueling intervals and relatively small (approximately 6% of the core per outage) fuel-replacement fraction in AGRs together lead to a smaller change in the antineutrino flux and spectrum from the beginning to the end of cycle compared to other reactor types.

We provide this description of the evolution of the AGR antineutrino spectrum to permit reliable assessments of the performance of antineutrino-based monitoring concepts for nonproliferation-oriented monitoring of AGRs, including estimations of the sensitivity of the antineutrino rate and spectrum to the fuel content and the reactor thermal power. The antineutrino spectral variation that we present, while specific to AGRs, also helps to provide insight into the likely behavior of other reactor designs that use a similar batch-refueling approach, such as RBMK, CANDU, and other reactors.

ACKNOWLEDGMENTS

This work was performed under the auspices of the U.S. Department of Energy by the Lawrence Livermore National Laboratory under Contract No. DE-AC52-07NA27344. R.M. acknowledges funding from his laboratory's internal research and development program. Those of us at the University of Liverpool acknowledge support by the Science and Technology Facilities Council (STFC) and the UK National Nuclear Laboratory for cofunding an Engineering and Physical Sciences Research Council (EPSRC) Next Generation Nuclear studentship. We would like to thank Sebin John and Daniel Gura of EDF Energy for their assistance in the production of the Hartlepool reactor data set.

[1] K. Eguchi *et al.* (collaboration KamLAND), First results from KamLAND: Evidence for reactor anti-neutrino disappearance, *Phys. Rev. Lett.* **90**, 021802 (2003).

[2] Y. Abe *et al.* (Double Chooz Collaboration), Indication of reactor $\bar{\nu}_e$ disappearance in the Double Chooz experiment, *Phys. Rev. Lett.* **108**, 131801 (2012).

[3] A. A. Borovoi and L. A. Mikaelyan, Possibilities of the practical use of neutrinos, *Sov. At. Energy* **44**, 589 (1978).

[4] A. Bernstein, N. Bowden, A. Misner, and T. Palmer, Monitoring the thermal power of nuclear reactors with a prototype cubic meter antineutrino detector, *J. Appl. Phys.* **103**, 074905 (2008).

[5] F. P. An *et al.* (collaboration Daya Bay), Evolution of the reactor antineutrino flux and spectrum at Daya Bay, *Phys. Rev. Lett.* **118**, 251801 (2017).

[6] D. A. Dwyer, Antineutrinos from nuclear reactors: Recent oscillation measurements, *New J. Phys.* **17**, 025003 (2015).

[7] P. Huber, On the determination of anti-neutrino spectra from nuclear reactors, *Phys. Rev.* **C84**, 024617 (2011).

[8] C. L. Jones, A. Bernstein, J. M. Conrad, Z. Djurcic, M. Fallot, L. Giot, G. Keefer, A. Onillon, and L. Winslow, Reactor simulation for antineutrino experiments using DRAGON and MURE, *Phys. Rev. D* **86**, 012001 (2012).

[9] A. Bernstein, N. S. Bowden, and A. S. Erickson, Reactors as a source of antineutrinos: The effect of fuel loading and burnup for mixed oxide fuels, *Phys. Rev. Appl.* **9**, 014003 (2018).

[10] C. Matthews and T. S. Palmer, Calculation of the antineutrino source term during CANDU reactor startup, *Ann. Nucl. Energy* **54**, 67 (2013).

[11] O. A. Akindele, A. Bernstein, and E. B. Norman, Antineutrino monitoring of thorium reactors, *J. Appl. Phys.* **120**, 124902 (2016).

[12] K. Schreckenbach, Fundamental physics with slow neutrons, *Acta Phys. Hung.* **75**, 25 (1994).

[13] R. Mills, B. Slingsby, J. Coleman, R. Collins, G. Holt, C. Metelko, and Y. Schnellbach, A simple method for estimating the major nuclide fractional fission rates within light water and advanced gas cooled reactors, *Nucl. Eng. Technol.* **52**, 2130 (2020).

[14] R. Mills and B. Slingsby, Commercial nuclear reactor fractional fission rate database from FISPIN 10A calculations for AGR, PWR and BWR, <https://data.mendeley.com/datasets/92523hssgv/2> (2020).

[15] P. Huber and P. Jaffke, Neutron capture and the antineutrino yield from nuclear reactors, *Phys. Rev. Lett.* **116**, 122503 (2016).

[16] S. Tarlton, *Nuclear Engineering International: World Nuclear Industry Handbook* (Unwin Brothers, Woking, Surrey, United Kingdom, 2003).

[17] E. Somasundaram, T. Palmer, and A. Soldatov, Benchmarked, three-dimensional antineutrino source term calculations of light water reactors for nonproliferation applications, *Nucl. Technol.* **179**, 160 (2012).

[18] E. Somasundaram, Master's thesis, School of Nuclear Science and Engineering, Oregon State University, 2011.

[19] <https://www.edfenergy.com/energy/power-stations/hartlepool/xenah>.